Role of the ATP Synthase α-Subunit in Conferring Sensitivity to Tentoxin†

Ward C. Tucker,‡,§ Ziyun Du,|| Ray Hein,‡ Zippora Gromet-Elhanan,|| and Mark L. Richter*,‡

Department of Molecular Biosciences, The University of Kansas, Lawrence, Kansas 66045, and the Department of Biological Chemistry, Weizmann Institute of Science, Rehovot 76100, Israel

Received March 13, 2001

ABSTRACT: Tentoxin, produced by phytopathogenic fungi, selectively affects the function of the ATP synthase enzymes of certain sensitive plant species. Binding of tentoxin to a high affinity ($K_i \approx 10$ nM) site on the chloroplast F_1 (CF_1) strongly inhibits catalytic function, whereas binding to a second, lower affinity site ($K_d > 10$ μM) leads to restoration and even stimulation of catalytic activity. Sensitivity to tentoxin has been shown to be due, in part, to the nature of the amino acid residue at position 83 on the catalytic β subunit of CF_1. An aspartate in this position is required, but is not sufficient, for tentoxin inhibition. By comparison with the solved structure of mitochondrial F_1 [Abrahams, J. P., Leslie, A. G. W., Lutter, R., and Walker, J. E. (1994) *Nature 370*, 621−628], Asp83 is probably located at an interface between α and β subunits on CF_1 where residues on the α subunit could also participate in tentoxin binding. A hybrid core F_1 enzyme assembled with β and γ subunits of the tentoxin-sensitive spinach CF_1, and an α subunit of the tentoxin-insensitive photosynthetic bacterium *Rhodospirillum rubrum* F_1 (RrF_1), was stimulated but not inhibited by tentoxin [Tucker, W. C., Du, Z., Gromet-Elhanan, Z. and Richter, M. L. (2001) *Eur. J. Biochem. 268*, 2179−2186]. In this study, chimeric α subunits were prepared by introducing short segments of the spinach CF_1 α subunit from a poorly conserved region which is immediately adjacent to β-Asp83 in the crystal structure, into equivalent positions in the RrF_1 α subunit using oligonucleotide-directed mutagenesis. Hybrid enzymes containing these chimeric α subunits had both the high affinity inhibitory tentoxin binding site and the lower affinity stimulatory site. Changing β-Asp83 to leucine resulted in loss of both inhibition and stimulation by tentoxin in the chimeras. The results indicate that tentoxin inhibition requires additional α residues that are not present on the RrF_1 α subunit. A structural model of a putative inhibitory tentoxin binding pocket is presented.

The F_OF_1 ATP synthases found in the inner mitochondrial membranes, the chloroplast thylakoid membranes, and bacterial cytoplasmic membranes, couple the movement of protons down an electrochemical proton gradient to the synthesis of ATP. The general structure of these enzymes is highly conserved, consisting of F_O, the membrane-spanning proton channel, and F_1, the peripheral membrane sector, which contains the catalytic sites for reversible ATP synthesis. The catalytic F_1 portion is comprised of five different polypeptide subunits designated α to ϵ in order of decreasing molecular weight with a stoichiometry of $\alpha_3\beta_3\gamma_1\delta_1\epsilon_1$. The X-ray crystal structure of the mitochondrial F_1 (MF_1)[1] at 2.8-Å resolution (*1*) defined the three-dimensional structures of alternating α and β subunits as forming a closed hexamer with a portion of the γ subunit embedded in the central cavity. Six nucleotide binding sites are located one at each of the six α/β interfaces. Three catalytic sites, located primarily on the β subunits, were found to exist in three different conformational states. This asymmetric feature is compatible with the *binding change* mechanism which proposed that the catalytic sites interconvert between three different conformational states during ATP synthesis via energy-dependent affinity changes in substrate binding and product release (*2*, *3*). Several recent studies of isolated F_1 (*4*, *5*) or F_OF_1 (*6*−*8*) have suggested that this is achieved by rotation of the γ subunit relative to the $\alpha_3\beta_3$ subassembly.

Tentoxin, a cyclic tetrapeptide [cyclo L-leucyl-*N*-methyl−methyl-(*z*)-dehydro-phenylalanyl-glycyl-*N*-methyl-alanyl], produced by phytopathogenic fungi from the *Alternaria* genus acts as a highly specific, uncompetetive inhibitor with respect to nucleotide substrates of the chloroplast ATP synthase (*9*−*11*). Tentoxin is known to interact directly with CF_1 and appears to block catalytic function by blocking cooperative release of tightly bound nucleotides from the enzyme (*12*). Binding of one molecule of tentoxin to a high affinity ($K_d < 10^{-8}$ M) site on CF_1 results in almost total inhibition of its ATPase activity (*11*, *13*−*15*). Further binding of tentoxin to one (*15*−*17*) or two (*14*) lower affinity ($K_d > 10^{-6}$ M) sites on CF_1 reactivates and actually stimulates the inhibited enzyme. Similarly, low concentrations of tentoxin fully inhibit ATP synthesis by thylakoid membranes and higher concentrations partially restore ATP synthesis activity (*18*).

† This work was supported in part by grants from the United States-Israel Binational Science Foundation (Jerusalem, Israel) and from the United States Department of Agriculture (NRICGP 9801577).

* To whom correspondence should be addressed.

‡ Department of Molecular Biosciences.

§ Recipient of a fellowship under National Institutes of Health Predoctoral Training Grant GM08545.

|| Department of Biological Chemistry.

[1] Abbreviations: MF_1, CF_1, EcF_1, and RrF_1, F_1-ATPases from mitochondria, chloroplasts, *E. coli*, and *R. rubrum*, respectively; α^C, β^C, and γ^C, α, β, and γ subunits of CF_1; α^R and β^R, α and β subunits of RrF_1; WT, wild-type; Tricine, *N*-[2-hydroxy-1,1-bis(hydroxymethyl)-ethyl]glycine; PCR, polymerase chain reaction; HPLC, high-performance liquid chromatography.

10.1021/bi0105227 CCC: $20.00
Published on Web 06/02/2001

Avni et al. (*19*) identified a correlation between tentoxin sensitivities of different *Nicotiana* species and the type of amino acid residue present at position 83 in the β amino acid sequence. Species with aspartate in this position were tentoxin sensitive whereas those with glutamic acid were tentoxin resistant. Moreover, mutation of Glu83 to Asp83 in the β subunit of tentoxin-resistant *Chlamydomonas reinhardtii* induced tentoxin sensitivity in that organism (*19, 20*). Therefore, at least part of the N-terminal region of the β subunit is involved in conferring tentoxin sensitivity. It was suggested that Asp83 is either the tentoxin receptor itself or that it interacts directly with the tentoxin receptor (*19*). However, several observations suggest that tentoxin binding involves more than Asp83. First, the β subunit of the *Escherichia coli* F_1 contains aspartate at the equivalent of position 83 yet is not sensitive to tentoxin (*21*). Second, a hybrid enzyme formed by complementing a β-less strain of *E. coli* with spinach β subunit was shown to be resistant to tentoxin (*21*). Third, it was observed that isolated CF_1 β (β^C) subunits were unable to compete effectively with CF_1 for high-affinity tentoxin binding (*12*). Similarly, a preparation of reconstitutively active $\alpha_3\beta_3$ hexamer isolated from CF_1 was also unable to compete effectively with CF_1 for tentoxin binding (*22*). These observations, together with the fact that the core $\alpha_3\beta_3\gamma$ complex of CF_1, lacking the δ and ϵ subunits, is fully sensitive to tentoxin inhibition, led to the suggestion that tentoxin binds at an $\alpha\beta$ interface of a special $\alpha\beta$ subunit pair within the CF_1 complex (*22*). The unique conformation of the special $\alpha\beta$ pair is assumed to be induced via an asymmetric interaction between the γ subunit and the $\alpha_3\beta_3$ hexamer.

We recently described a method of reconstituting β^C subunits along with either α^R or α^C subunits to chromatophores from the photosynthetic bacterium *Rhodospirillum rubrum* which had been partially depleted of both their α and β subunits by LiCl treatment (*23*). This allowed us to examine the effects of several β^C mutations on tentoxin sensitivity in the presence of either the bacterial or the chloroplast α subunits. The wild-type β^C subunit was found to confer tentoxin sensitivity on the normally tentoxin resistant *R. rubrum* chromatophores only in the presence of the α^C subunit but not the α^R subunit. This clearly demonstrated that both the α and β subunits are involved in conferring sensitivity to inhibition by tentoxin upon the enzyme. Irrespective of which α subunit was present, hybrid chromatophores containing any one of three β^C mutants with Asp83 substituted with glutamate, alanine or leucine, were completely insensitive to tentoxin. This indicates an absolute requirement for Asp in position 83 of β^C which is consistent with a direct binding interaction between Asp83 and tentoxin (*19, 20*). In another recent study (*24*), a hybrid F_1 containing the α subunit from RrF_1 and the CF_1 β and γ subunits was shown to contain the stimulatory binding site for tentoxin but not the inhibitory site, indicating that the two sites have different structural requirements. However, exchange of Asp83 for Leu eliminated stimulatory tentoxin binding indicating that the stimulatory and inhibitory sites have at least some structural features in common (*24*).

In this study, we have incorporated chimeric α subunits into the photosynthetic hybrid RrF_1/CF_1 enzyme to further examine the structural requirements for the binding of tentoxin. The results have led to the identification of a region of the α subunit which, together with part of the β subunit, is involved in forming the inhibitory tentoxin binding site.

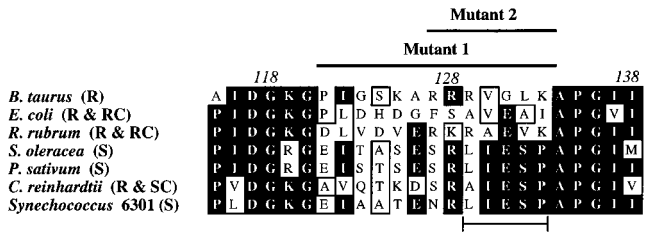

FIGURE 1: Sequence alignment of ATP synthase α subunits with known sensitivities to tentoxin. Sequences of a short segment of the α subunits from seven species with known tentoxin sensitivities were aligned using MacVector (Oxford Molecular Group). The species are classified as being resistant (R) or sensitive (S) to tentoxin inhibition (*19, 21, 33, 37*−*39*) $(MF_1)^2$. An additional distinction has been made based on previous studies which have examined tentoxin sensitivity of hybrid enzymes containing the β subunit from tentoxin-sensitive chloroplasts. The F_1 enzymes which are normally tentoxin resistant either became tentoxin sensitive (SC) or remained insensitive to tentoxin (RC) when the CF_1 β was present (*19, 21, 23*). Heavy lines have been drawn above two segments of residues which were used to create chimeric α subunits. In mutant 1 (121−133) and mutant 2 (127−133), the *S. oleracea* α sequences were inserted in place of the corresponding sequences of the *R. rubrum* α subunit. The segment of five residues which is underlined is located within 10 Å of Asp83 on the β subunit of bovine MF_1 as determined by examining the crystal structure (*1*). Chloroplast numbering is shown.

EXPERIMENTAL PROCEDURES

Materials. CF_1 lacking the δ and ϵ subunit, $\alpha^C{}_3\beta^C{}_3\gamma^C$, was reconstituted from native α and β subunits and recombinant, refolded γ subunit as previously described (*22, 25*). β^C (*26*), β^{D83L} (*23*), and γ^C (*25*) were expressed as inclusion bodies in *E. coli* BL21(DE3)/pLysS cells grown to steady state at 37 °C. ATP (grade II) and tentoxin were purchased from Sigma. Tentoxin was dissolved in ethanol or methanol to a final concentration of 5 mM and stored at −80 °C. All other chemicals were the highest quality reagent grade available.

Preparation of α *Subunit Chimeras.* The $RrF_1\alpha$ gene was amplified from the previously described pTZα plasmid (*27*) and ligated into the pET3a expression vector. The entire α gene sequence and the proper placement in the vector were verified by the fluorescent dideoxy method (*28*). Upon transformation of the BL21(DE3)/pLysS strain with the plasmid, designated pET3a-$RrF_1\alpha$, α^R was expressed exclusively as inclusion bodies. Two separate α chimeras were prepared, each containing a short sequence of amino acids from the spinach α^C subunit in place of the equivalent segment in α^R (Figure 1). Chimeras were constructed by enzymatic amplification of the expression plasmid pET3a-$RrF_1\alpha$ using previously described inverse PCR methods (*23, 26*). The primers employed (synthesized and 5′-phosphorylated by Macromolecular Resources, Colorado State University) had abutting 5′ termini allowing for replication of the whole plasmid along with the mutation. For the first mutation, designated α^{M1}, the reverse and forward primers were 39 and 35 nucleotides long, respectively, with a priming area corresponding to positions +339 to +412 of the $RrF_1\alpha$ gene. The 5′ sequence of the reverse primer was GATTCAGAAGCTGTAATTTC and the 5′ sequence of the forward

[2] Z. Gromet-Elhanan, unpublished experiments.

primer was TCGGTTAATTGAGTCTCCA such that the α^R amino acid sequence DLVDVERKRAEVK was replaced by the spinach α^C sequence EITASESRLIESP. The second mutation, α^{M2}, was generated in a similar manner with a reverse primer of 28 nucleotides and a forward primer of 27 nucleotides corresponding to positions +358 to +412 of the $RrF_1\alpha$ gene. The 5′ sequence of the reverse primer (TTAACCGAGA) and the forward primer (TTGAATCACCA) allowed for the substitution of the α^R amino acid sequence RKRAEVK for the spinach chloroplast sequence SRLIESP. Oligonucleotides were generated with the aid of the program Primer Designer (SciEd Software).

PCR was carried out in 50 μL of *Pfu* DNA polymerase reaction buffer also containing 4 mM total $MgSO_4$, 20 pmol of each primer, 0.4 mM dNTPs, 60 ng of the pET3a-$RrF_1\alpha$ plasmid DNA, and 2.5 units of cloned *Pfu* DNA polymerase (Stratagene). All components were mixed on ice and placed in a GenAmp PCR System 2400 (Perkin-Elmer) prewarmed to 94 °C. The cycling parameters were 94 °C, 1 min; 65 °C, 1 min; and 72 °C, 12 min, for 25 cycles. PCR products were purified by gel electrophoresis followed by electroelution using an ISCO micro trap. The eluted DNA was precipitated with ethanol and circularized by incubating the eluted DNA with 3 units of T4 DNA ligase (Promega) in T4 ligase buffer overnight at room temperature. The plasmid was then transformed into competent *E. coli* XL1-blue cells (Stratagene). Cloned plasmid was isolated using boiling lysis followed by 2-propanol and ethanol precipitation and transformed into the expression host *E. coli* BL21(DE3)/pLysS (Stratagene). The mutations were confirmed by sequencing the entire α gene using the fluorescent dideoxy method (*28*).

Reconstitution of Hybrid, Chimeric F_1 Enzymes. Washed inclusion bodies containing the expressed proteins in highly purified forms (>80% homogeneous) were prepared from *E. coli* cells as described previously (*26*). Inclusion bodies containing the α^R or α mutants M1 and M2, β^C, and γ^C were individually solubilized in refolding buffer containing 3 M guanidine-HCl, 50 mM Tris-HCl (pH 8), 50 mM $MgCl_2$, 50 mM ATP, 50 mM DTT, and 20% glycerol. After a 1 h incubation at 4 °C, insoluble material was removed by centrifugation at 30000*g* for 30 min before mixing of the subunits and further dilution with refolding buffer to give final concentrations of 50, 50, and 30 μg/mL for α^R, β^C, and γ^C, respectively. The mixture was dialyzed at 22 °C overnight against 50 mM Tris-HCl (pH 8), 50 mM NaCl, and 20% glycerol prechilled to 4 °C. Warming the buffer during dialysis was essential for efficient reconstitution. The dialyzed samples were then concentrated to 4−8 mg/mL before being subjected to size-exclusion HPLC on a Superdex-200 column (Pharmacia). The $\alpha_3\beta_3\gamma$ peak was collected, pooled, and concentrated to 1−1.5 mg/mL. About 5% of the recombinant proteins were recovered from the column as an assembled, apparently homogeneous hybrid core enzyme complex which could be stored at −80 °C indefinitely without loss of catalytic activity (*24*).

Activity Assays of Hybrid, Chimeric F_1 Enzymes. The Ca^{2+}-dependent ATP hydrolysis activities were measured for 5 min at 37 °C in the presence of 50 mM Tricine-NaOH (pH 8.0), 4 mM ATP, 4 mM $CaCl_2$, 50 mM NaCl, and 5 μg of enzyme. Mg^{2+}-dependent ATP hydrolysis was measured for 5 min at 37 °C in the presence of 50 mM Tris-HCl (pH 8.0), 4 mM ATP, 2 mM $MgCl_2$, 50 mM NaCl, and 5−10 μg of enzyme. P_i release was determined spectrophotometrically (*29*). For tentoxin sensitivity assays, assembled enzymes were preincubated in the reaction mixture minus ATP with the indicated amount of tentoxin or, in controls, with an identical amount of the alcohol used to solubilize the inhibitor. After a 12 min incubation at 22 °C and then 3 min at 37 °C, the reaction was initiated by the addition of 4 mM ATP.

Other Procedures. Protein concentrations were determined by the method of Lowry et al. (*30*) or by the method of Bradford (*31*) using bovine serum albumin as standard. SDS−PAGE was carried out on NOVEX Pre-Cast 10−20% Tris-Glycine gradient gels.

RESULTS

Preparation of Chimeric α Subunits. Figure 1 shows an alignment of a short section of the amino acid sequences of F_1 α subunits from several different species. The group of five residues which is underlined (129−133) is within 10 Å of the amino acid at position 83 on the β subunit in the crystal structure of MF_1 (*1*). These residues happen to lie in a relatively poorly conserved segment of the α subunit, located between residues 121 and 133. The variability of the sequence within this region makes it a good candidate region for containing sequence differences which might determine susceptibility of the respective F_1 enzymes to tentoxin binding and inhibition. To examine this possibility, two chimeric α subunits were prepared in which selected regions of the tentoxin resistant α^R subunit were substituted with regions of the tentoxin sensitive spinach α^C subunit. The sequences substituted are those indicated in Figure 1 as mutant 1, which encompasses the entire poorly conserved region, and mutant 2 which encompasses a more limited, although overlapping, segment of α between residues 127 and 133. Chimeric α subunits were prepared by oligonucleotide-direct mutagenesis in conjunction with inverse PCR amplification of the pET3a-$RrF_1\alpha$ plasmid containing the full-length gene encoding the *R. rubrum* F_1 α subunit. Overexpression of the chimeric α subunit genes in *E. coli* resulted in production of full length α subunits which were packaged in inclusion bodies within the overexpressing cells.

Assembly and Assay of CF_1/RrF_1 Hybrids. Each of the two mutant proteins was solubilized from inclusion bodies using guanidine-HCl, folded, and assembled with the β^C and γ^C subunits and the assembly was purified by HPLC as described in the Experimental Procedures. The yields and polypeptide profiles (Figure 2) of the resulting hybrid F_1 enzymes containing the chimeric α subunits were indistinguishable from those of the hybrid containing the wild-type α^R subunit. Thus the mutations did not cause any obvious effects on protein folding and assembly. Table 1 compares the ATPase activities of the hybrid enzymes to those of the wild-type hybrid. The CaATPase activity of the chimera containing mutant 1, $\alpha^{M1}{}_3\beta^C{}_3\gamma^C$, was similar to that of the wild-type hybrid whereas that of the chimera containing mutant 2, $\alpha^{M2}{}_3\beta^C{}_3\gamma^C$, was significantly lower. The reason for the difference is unclear. In contrast, the MgATPase and sulfite-stimulated MgATPase activities of both mutants were similar to those of the wild-type hybrid. All three hybrid enzymes showed the expected 5−6-fold stimulation by sulfite ions which results from relief of inhibition of ATPase activity caused by free Mg^{2+} (*32*).

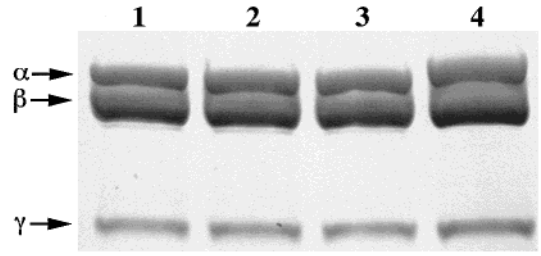

FIGURE 2: SDS−PAGE profile of purified, chimeric $\alpha_3\beta_3\gamma$ assemblies. Wild-type or chimeric α subunits were folded along with the β^C and γ^C subunits and purified by HPLC as described in the Experimental Procedures. Electrophoresis was performed on a 10−20% Tris-glycine gel before staining with Coomassie Brilliant Blue R. Each lane contained 4 μg of protein. Lanes 1−3, $\alpha^R{}_3\beta^C{}_3\gamma^C$ assemblies containing wild-type α^R, α^{M1}, or α^{M2}, respectively; lane 4, reconstituted $\alpha^C{}_3\beta^C{}_3\gamma^C$.

Table 1: ATPase Activities of Wild-Type and Mutant Hybrid Complexes[a]

	(μmol of P_i/min/mg of protein)		
	MgATPase		
complex	−sulfite	+sulfite	CaATPase
$\alpha^R{}_3\beta^C{}_3\gamma^C$	1.63 ± 0.29	9.3 ± 0.6	8.7 ± 0.7
$\alpha^{M1}{}_3\beta^C{}_3\gamma^C$	1.52 ± 0.05	10.8 ± 0.8	9.6 ± 1.0
$\alpha^{M2}{}_3\beta^C{}_3\gamma^C$	1.27 ± 0.10	8.8 ± 0.2	3.7 ± 0.7

[a] A total of 5−10 μg of the indicated protein preparation were assayed as described in Experimental Procedures. Mg-ATPase activities are given in the presence or absence of 50 mM sodium sulfite. Standard deviation is shown for four separate determinations.

Tentoxin Inhibition of Hybrids Containing α Chimeras. The effects of tentoxin on the CaATPase activities of the hybrid enzymes are shown in Figure 3A. Whereas the enzyme containing the wild type α was only slightly inhibited (<20%) by tentoxin concentrations up to 100 μM, the two mutant hybrids were strongly inhibited (60−75%) with half-maximal inhibition at 1−2 μM. This is in contrast to the core CF_1 enzyme ($\alpha^C{}_3\beta^C{}_3\gamma^C$) which is inhibited half-maximally at a 50 to 100 times lower concentration (~20 nM). A similar result was obtained with the sulfite-stimulated MgATPase activities of the mutant hybrids (Figure 3B). In this case, however, the contrast between wild-type and mutant hybrids was even more marked. The mutants were maximally inhibited to 70−80% while the wild-type hybrid was apparently not affected by tentoxin. Thus the introduction of the spinach chloroplast α sequence into the *R. rubrum* α caused the enzyme to become sensitive to inhibition by tentoxin. Both of the mutants conferred tentoxin sensitivity upon the enzyme and the concentration dependence for inhibition and stimulation was essentially identical for both. This indicates that only the C-terminal part of the poorly conserved segment, contained in mutant 2 of α as shown in Figure 1, is specifically required for high affinity tentoxin binding to the inhibitory site.

The ATPase activity of the control $\alpha^C{}_3\beta^C{}_3\gamma^C$ complex (Figure 3B, diamonds) recovers from its inhibited state when the tentoxin concentration increases above 1 μM. Interestingly, the activities of the two mutants showed the same pattern, both being inhibited at lower tentoxin concentrations and stimulated at higher concentrations. The much lower MgATPase activities of the assemblies in the absence of stimulating sulfite ions behaved similarly (Figure 4). In this case, however, the activity not only recovered at higher tentoxin concentrations, but it actually became stimulated to rates in excess of the starting rates. This overstimulation phenomenon has been observed elsewhere for partially activated CF_1 (*15*, *16*) and continues up to saturating concentrations of tentoxin (>1 mM).

The control hybrid assembly which contained the wild type α^R subunit is not inhibited by low concentrations of tentoxin but is stimulated at higher concentrations (Figure 4). This stimulation, which was described for the first time recently (*24*), depends on the presence of the β^C subunit. Since it occurs in the absence of an inhibitory response it indicates that there is a different protein structural requirement on CF_1 for the inhibitory and stimulatory effects of tentoxin (*24*). The stimulatory response of the wild-type hybrid was observed

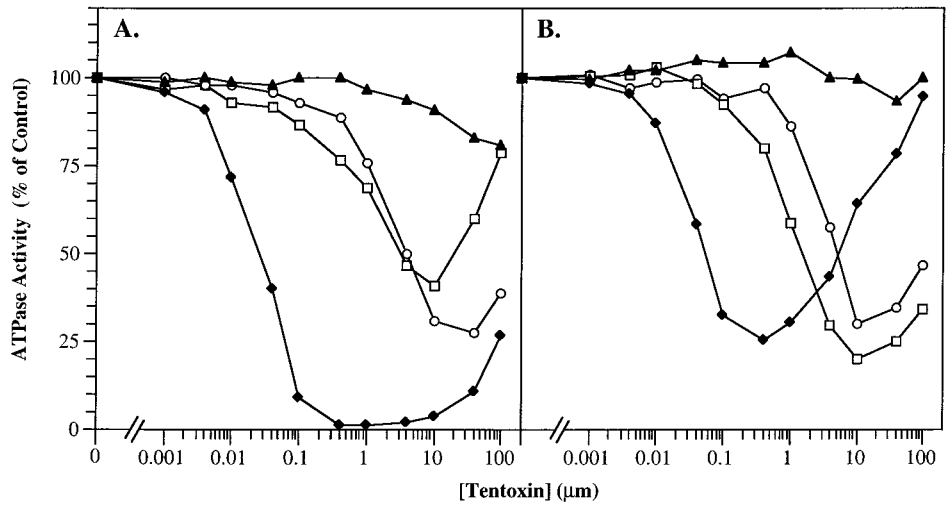

FIGURE 3: Effect of tentoxin on the Ca-ATPase and sulfite-stimulated Mg-ATPase activities of CF_1-$\alpha^C{}_3\beta^C{}_3\gamma^C$ and the hybrid $\alpha^R{}_3\beta^C{}_3\gamma^C$ complexes containing the wild-type or chimeric α subunits. A total of 5 μg of $\alpha^C{}_3\beta^C{}_3\gamma^C$ (◆), $\alpha^R{}_3\beta^C{}_3\gamma^C$ (▲), $\alpha^{M1}{}_3\beta^C{}_3\gamma^C$ (○), and $\alpha^{M2}{}_3\beta^C{}_3\gamma^C$ (□) were incubated in the presence of the indicated concentration of tentoxin at 22 °C for 12 min then at 37 °C for 3 min before the addition of 4 mM ATP to initiate Ca-ATP hydrolysis (panel A) or sulfite-stimulated Mg-ATP hydrolysis (panel B) as described in the Experimental Procedures. Control Ca-ATPase activites in the absence of tentoxin were 8.7, 7.8, 8.1, and 2.4 μmol of P_i/min/mg of $\alpha^C{}_3\beta^C{}_3\gamma^C$, $\alpha^R{}_3\beta^C{}_3\gamma^C$, $\alpha^{M1}{}_3\beta^C{}_3\gamma^C$, or $\alpha^{M2}{}_3\beta^C{}_3\gamma^C$ respectively. Control sulfite-stimulated (50 mM Na_2SO_3) Mg-ATPase activites in the absence of tentoxin were 20.4, 8.4, 11.6, and 8.9 μmol of P_i/min/mg of $\alpha^C{}_3\beta^C{}_3\gamma^C$, $\alpha^R{}_3\beta^C{}_3\gamma^C$, $\alpha^{M1}{}_3\beta^C{}_3\gamma^C$, and $\alpha^{M2}{}_3\beta^C{}_3\gamma^C$ respectively.

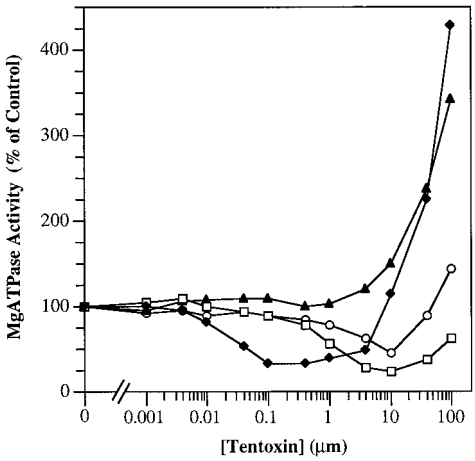

FIGURE 4: The effect of tentoxin on the Mg-ATPase activities of CF_1-$\alpha^{C}{}_3\beta^{C}{}_3\gamma^{C}$ and the hybrid $\alpha^{R}{}_3\beta^{C}{}_3\gamma^{C}$ complexes containing the wild-type or chimeric α subunits. A total of 10 μg of each complex was incubated with the indicated amount of tentoxin as described in the legend to Figure 3 before the initiation of MgATP hydrolysis in the absence of sulfite. Symbols are the same as in Figure 3 [$\alpha^{C}{}_3\beta^{C}{}_3\gamma^{C}$ (◆), $\alpha^{R}{}_3\beta^{C}{}_3\gamma^{C}$ (▲), $\alpha^{M1}{}_3\beta^{C}{}_3\gamma^{C}$ (○), and $\alpha^{M2}{}_3\beta^{C}{}_3\gamma^{C}$ (□)]. Control activites in the absence of tentoxin were 1.3, 1.2, 1.6, and 1.4 μmol of P_i/min/mg of $\alpha^{C}{}_3\beta^{C}{}_3\gamma^{C}$, $\alpha^{R}{}_3\beta^{C}{}_3\gamma^{C}$, $\alpha^{M1}{}_3\beta^{C}{}_3\gamma^{C}$, and $\alpha^{M2}{}_3\beta^{C}{}_3\gamma^{C}$, respectively.

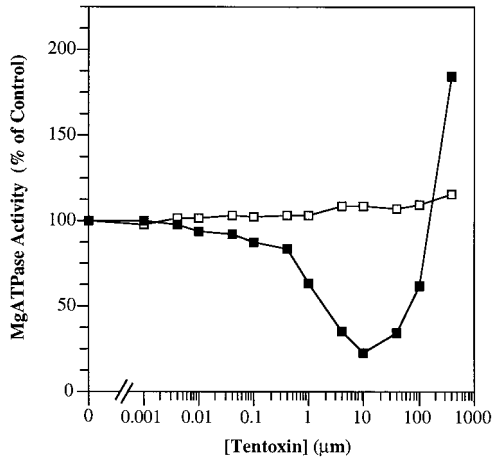

FIGURE 5: Asp83 of CF_1 β is essential for tentoxin inhibition in the hybrid chimeric enzymes. A total of 10 μg of $\alpha^{M2}{}_3\beta^{C}{}_3\gamma^{C}$ (■) or $\alpha^{M2}{}_3\beta^{C-D83L}{}_3\gamma^{C}$ (□) were incubated with the indicated amount of tentoxin as described in Figure 3 before the initiation of MgATP hydrolysis in the absence of sulfite. Control activities in the absence of tentoxin were 1.6 and 1.9 μmol of P_i/min/mg of $\alpha^{M2}{}_3\beta^{C}{}_3\gamma^{C}$ or $\alpha^{M2}{}_3\beta^{C-D83L}{}_3\gamma^{C}$, respectively.

when the enzyme was turning over at very low rates as in the non-sulfite-stimulated ATPase activity shown in Figure 4. Under conditions where the enzyme was turning over at high rates, which was the case for the CaATPase or sulfite-stimulated MgATPase activities of the wild-type hybrid shown in Figure 3, the stimulatory response was not observed at the tentoxin concentrations tested. One possible explanation for this effect is that the hybrid enzyme containing the wild-type RrF_1 α does bind tentoxin into the inhibitory binding site but with a very low affinity such that the inhibitory and stimulatory effects mask each other. A thorough evaluation of such effects was precluded because of the limited solubility of tentoxin in the millimolar range (*15*).

The results presented in Figure 5 show the affect of mutating Asp83 to Leu on the β^{C} subunit on the sensitivity

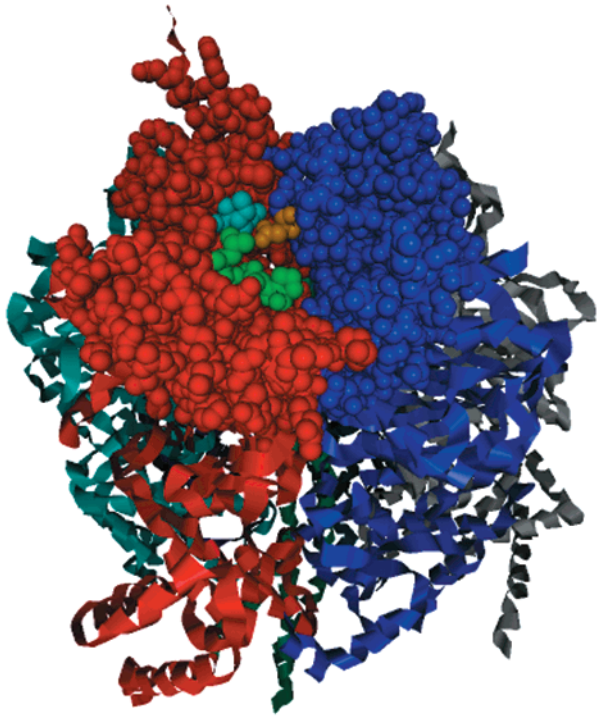

FIGURE 6: Putative binding pocket for tentoxin is located at an α/β interface of CF_1. A single α subunit is shown in red along with a single β subunit in blue. The space-filled regions are the N-terminal β barrel domains of the α and β subunits which form a tightly packed ring at the top of the αβ hexamer. Asp83 of β is shown in khaki. Residues 129−133 of α are shown in green (see Figure 1) and conserved residues Gly51 and Ile95 of α are shown in light blue. The model was generated with Look (Molecular Applications group) using a spinach CF_1 homology model of the bovine MF_1 structure.

to tentoxin of the hybrid assembly containing the chimeric mutant 2 α subunit. This mutation was shown previously to block the inhibitory action of tentoxin on hybrid *R. rubrum* chromatophores containing the α and β subunits of CF_1 (*23*) and to block the stimulatory response to tentoxin of the $\alpha^{R}{}_3\beta^{C}{}_3\gamma^{C}$ hybrid assembly (*24*). Changing Asp83 to Leu completely abolished both the inhibitory and stimulatory responses to tentoxin in the chimeric assembly (Figure 5), indicating that the induced sensitivity to tentoxin resulted from the same type of interaction between tentoxin and the hybrid F_1 subunits as that which occurs in CF_1.

DISCUSSION

Model of the Inhibitory Tentoxin Binding Site at an αβ Interface. Figure 6 shows part of the three-dimensional structure of an αβ pair derived from a homology model of CF_1 α, β, and γ subunits based on the beef heart MF_1 structure. The residue Asp83 (colored khaki in Figure 6) is located on the N-terminal β-barrel structure of the β subunit near the top of the molecule. The top is defined as the end which is furthest away from the membrane in the F_OF_1 complex. The N-terminal domains of three such αβ pairs are tightly bound together to form a ring which probably provides most of the stabilizing energy holding the F_1 hexamer together (*1*). Asp83 is at the immediate interface of the αβ pair, the same interface that creates the catalytic nucleotide binding sites which are about 30 Å away toward the bottom of the molecule (*1*). Asp83 is oriented away from

the β N-terminus and into a depression or pocket which is formed by residues on both the α and β subunits. The entrance to the pocket is about 12 Å across which is large enough to accommodate tentoxin. Such a pocket has also been noted elsewhere (*15*). The residues colored in green in Figure 6 (α residues 129−133) line one edge of the pocket on the α subunit side. These residues are the same ones which are underlined in Figure 1 and are present in both M1 and M2 α chimeras.

The location of β-Asp83 and the α residues 129−133 within the pocket and the fact that changing these residues alters the response to inhibition by tentoxin, strongly suggest that tentoxin binds within the pocket. It was shown previously that exchanging Asp83 for Glu, Ala, or Leu in each case resulted in complete loss of the inhibitory response to tentoxin (*23*). These results implied that both the size and the charge on the residue at position 83 are critical factors in determining tentoxin sensitivity. One possibility is that Asp83 provides an essential hydrogen bonding ligand to tentoxin. In the CF_1 homology model, Asp83 forms hydrogen bonds with Gly51 and Ile95 on the α subunit, shown in blue in Figure 6. These two α residues are conserved in all of the F_1 species listed in Figure 1, including the tentoxin-resistant *E. coli* F_1 (EcF_1) and RrF_1. In RrF_1, as in MF_1, the residue equivalent to β^C−Asp83 is replaced with Glu. The bulkier side chain of Glu is oriented toward the outside of the pocket where it would be unable to interact directly with tentoxin. This would explain, at least in part, why RrF_1 (*33*) and MF_1[2] are not sensitive to tentoxin. But EcF_1, which contains the equivalent β-Asp61, is also resistant to inhibition by tentoxin (*21*) as is the hybrid $\alpha^R\beta^C\gamma^C$ (Figure 3). These results have suggested the involvement of additional α^C residues in the tentoxin binding pocket. The observation that introducing either of the two chimeric α subunits into the hybrid F_1 generated a similar tentoxin sensitivity indicates that the structural element responsible for this inhibition lies within the 127−133 sequence shared by M1 and M2. However, since the inhibitory binding of tentoxin to both hybrid enzymes containing the chimeric α subunits occurred with about a 30-fold lower apparent affinity than in CF_1, additional α^C residues besides those highlighted in Figure 6 might be required for attaining the full tight binding of tentoxin.

During the preparation of this manuscript, the structure of the $\alpha_3\beta_3$ hexamer of CF_1 at 3.2 Å resolution was published (*34*). The structure confirmed the overall properties of the tentoxin binding pocket described here but suggested a different involvement for Asp83 in conferring sensitivity to tentoxin. The structure indicated that Asp83 on β is close enough to Arg297 on the adjacent α to form a salt link which may be necessary for conferring tentoxin sensitivity. The α-Arg297 is, however, a conserved residue in all of the F_1 species shown in Figure 1. It is thus present together with the β^C-Asp83 in the hybrid $\alpha^R\beta^C\gamma^C$ which is not inhibited by tentoxin (Figures 3 and 4), and in the M1 and M2 chimeras, which are sensitive to tentoxin inhibition (Figures 3-5). So the conserved α residues Gly51, Ile95, and Arg297, are not, in themselves, sufficient to provide the steric environment within the pocket necessary for the tight binding of tentoxin.

Structural Features on the α Subunit Are Required for Inhibition but Not Stimulation of the Enzyme by Tentoxin. The involvement of the F_1 α^C subunit in conferring sensitivity to inhibition by tentoxin was demonstrated earlier (*23*). The results presented in this study show for the first time a specific involvement of the α^C-127−133 segment in tentoxin inhibition (Figure 3). The structure of this segment is, however, not important for stimulation by tentoxin since stimulation appears also in the WT α^R containing hybrid (*24* and Figure 4) which lacks this segment (Figure 1) and is not inhibited by tentoxin. Both inhibition and stimulation are, however, dependent on β^C-Asp83 (Figure 5). These results indicate that inhibition and stimulation by tentoxin must be due to its binding to two similar, but not identical ($\alpha\beta$) sites on CF_1. The simultaneous binding of two molecules of tentoxin to the enzyme was indeed demonstrated using a radioactively labeled tentoxin analogue (*15*). Since the stimulation occurs even in the CF_1 $\alpha_3\beta_3$ hexamer (*35*, *36*), it is apparent that the low-affinity binding site does not depend on the asymmetric state of the enzyme which is induced by binding of the γ subunit (*12*, *35*). In contrast, the high affinity inhibitory binding site requires the presence of the γ subunit and coincides with the presence of γ-induced high affinity nucleotide binding sites in CF_1 (*12*).

The high affinity binding of tentoxin to CF_1 is known to interfere with a process of communication between different nucleotide binding sites which results in negative cooperativity with respect to nucleotide binding (*12*). Yet the tentoxin binding pocket, as indicated in Figure 6, is located at a considerable distance from the nucleotide binding sites. Thus, the N-terminal domains of the α and β subunits must undergo conformational changes that are critically coupled to nucleotide binding events at catalytic sites. Indeed, a conformational link between the N-terminal domain and the nucleotide binding domain on the β subunit was suggested in an earlier study (*21*). In that case, mutations at position 63 of the β subunit, which is located at the base of the N-terminal domain and immediately in contact with the nucleotide binding domain, interfered with nucleotide-driven conformational changes and resulted in the loss of ATP synthesis activity.

With the identity of the tentoxin binding site, molecular docking simulations can now be used in conjunction with site-directed mutagenesis experiments to probe the mechanism by which binding of tentoxin to one site on the enzyme inhibits the cooperative process while subsequent binding to a similar site results in activation. Tentoxin thus promises to be a valuable tool in delineating the nature and sequence of conformational events involved in intersite cooperativity in the F_OF_1 enzymes.

ACKNOWLEDGMENT

The authors are grateful to Dr. Siegfried Engelbrecht for kindly providing the atomic coordinates for the homology models of the CF_1 α, β, and γ subunits.

REFERENCES

1. Abrahams, J. P., Leslie, A. G. W., Lutter, R., and Walker, J. E. (1994) *Nature 370*, 621−628.
2. Boyer, P. D. (1993) *Biochim. Biophys. Acta 1140*, 215−250.
3. Boyer, P. D. (1997) *Annu. Rev. Biochem. 66*, 717−749.
4. Noji, H., Yasuda, R., Yoshida, M., and Kinosita, K. (1997) *Nature 386*, 299−302.
5. Omote, H., Sambonmatsu, N., Saito, K., Sambongi, Y., Iwamoto-Kihara, A., Yanagida, T., Wada, Y., and Futai, M. (1999) *Proc. Natl. Acad. Sci. U.S.A. 96*, 7780−7784.

6. Sambongi, Y., Iko, Y., Tanabe, M., Omote, H., Iwamoto-Kihara, A., Ueda, I., Yanagida, T., Wada, Y., and Futai, M. (1999) *Science 286*, 1722−1724.
7. Panke, O., Gumbiowski, K., Junge, W., and Engelbrecht, S. (2000) *FEBS Lett. 472*, 34−38.
8. Tsunoda, S. P., Aggeler, R., Noji, H., Kinosita, K. J., Yoshida, M., and Capaldi, R. A. (2000) *FEBS Lett. 470*, 244−248.
9. Arntzen, C. J. (1972) *Biochim. Biophys. Acta 283*, 539−542.
10. Steele, J. A., Uchytil, T. F., Durbin, R. D., Bhatnagar, P., and Rich, D. H. (1976) *Proc. Natl. Acad. Sci. U.S.A. 73*, 2245−2248.
11. Steele, J. A., Durbin, R. D., Uchytil, T. F., and Rich, D. H. (1978) *Biochim. Biophys. Acta 501*, 72−82.
12. Hu, N., Mills, D. A., Huchzermeyer, B., and Richter, M. L. (1993) *J. Biol. Chem. 268*, 8536−8540.
13. Dahse, I., Pezennec, S., Girault, G., Berger, G., Andre, F., and Liebermann, B. (1994) *J. Plant Physiol. 143*, 615−620.
14. Mochimaru, M., and Sakurai, H. (1997) *FEBS Lett. 419*, 23−26.
15. Santolini, J., Haraux, F., Sigalat, C., Moal, G., and AndrÈ, F. (1999) *J. Biol. Chem. 274*, 849−858.
16. Steele, J. A., Uchytil, T. F., and Durbin, R. D. (1978) *Biochim. Biophys. Acta 504*, 136−141.
17. Pinet, E., Gomis, J. M., Girault, G., Cavelier, F., Verducci, J., Noel, J. P., and AndrÈ, F. (1996) *Febs Lett. 395*, 217−220.
18. Sigalat, C., Pitard, B., and Haraux, F. (1995) *FEBS Lett. 368*, 253−256.
19. Avni, A., Anderson, J. D., Holland, N., Rochaix, J. D., Gromet-Elhanan, Z., and Edelman, M. (1992) *Science 257*, 1245−1247.
20. Hu, D., Fiedler, H. R., Golan, T., Edelman, M., Strotmann, H., Shavit, N., and Leu, S. (1997) *J. Biol. Chem. 272*, 5457−5463.
21. Chen, Z., Spies, A., Hein, R., Zhou, X., Thomas, B. C., Richter, M. L., and Gegenheimer, P. (1995) *J. Biol. Chem. 270*, 17124−17132.
22. Gao, F., Lipscomb, B., Wu, I., and Richter, M. L. (1995) *J. Biol. Chem. 270*, 9763−9769.
23. Tucker, W. C., Du, Z., Hein, R., Richter, M. L., and Gromet-Elhanan, Z. (2000) *J. Biol. Chem. 275*, 906−912.
24. Tucker, W. C., Du, Z., Richter, M. L., and Gromet-Elhanan, Z. (2001) *Eur. J. Biochem. 268*, 2179−2186.
25. Sokolov, M., Lu, L., Tucker, W., Gao, F., Gegenheimer, P. A., and Richter, M. L. (1999) *J. Biol. Chem. 274*, 13824−13829.
26. Chen, Z., Wu, I., Richter, M. L., and Gegenheimer, P. (1992) *FEBS Lett. 298*, 69−73.
27. Du, Z., and Gromet-Elhanan, Z. (1995) in *Photosynthesis: from Light to Biosphere* (Mathis, P., Ed.) pp 27−30, Kluwer Academic Publishers.
28. Averboukh, L., Douglas, S. A., Zhao, S., Lowe, K., Mahler, J., and Pardee, A. B. (1996) *Biotechniques 20*, 918−921.
29. Taussky, H. H., and Shorr, E. (1953) *J. Biol. Chem. 202*, 675−685.
30. Lowry, O. H., Rosenbrough, N. J., Farr, A. L., and Randall, R. J. (1951) *J. Biol. Chem. 193*, 265−275.
31. Bradford, M. (1976) *Anal. Biochem. 72*, 248−254.
32. Du, Z., and Boyer, P. D. (1990) *Biochemistry 29*, 402−407.
33. Weiss, S., McCarty, R. E., and Gromet-Elhanan, Z. (1994) *J. Bioenerg. Biomembr. 26*, 573−580.
34. Groth, G., and Pohl, E. (2001) *J. Biol. Chem. 276*, 1345−1352.
35. Gromet-Elhanan, Z., and Avital, S. (1992) *Biochim. Biophys. Acta 1102*, 379−385.
36. Sokolov, M., and Gromet-Elhanan, Z. (1996) *Biochemistry 35*, 1242−1248.
37. Ohta, Y., Yoshioka, T., Mochimaru, M., Hisabori, T., and Sakurai, H. (1993) *Plant Cell Physiol.* 523−529.
38. Selman, B. R., and Durbin, R. D. (1978) *Biochim. Biophys. Acta 502*, 29−37.
39. Fulton, N. D., Bollenbacher, K., and Templeton, G. E. (1965) *Phytophathology 55*, 49−51.

BI0105227